

Physical behaviour of slag in a 107 tonne ladle. Production scale experiments and theoretical simulation.

Carl Erik Grip *), **Lage Jonsson **)**

*) SSAB Tunnplåt Luleå, S-97188 Luleå, Sweden **) MEFOS, Luleå, Sweden

Abstract

The combined movement of steel, slag and gas in a ladle has been studied with the aid of a multiphase CFD model and measurements in production scale. Comparison of model data and measurements in a production ladle has been carried out for three cases: The "open-eye" created during gas stirring, the mixing of top-slag during gas stirring in the CAS-OB and finally for studying sculling phenomena. It was found that the simulated "open-eye" appears as a central slag free zone with a surrounding "splash-zone" characterized by that steel is found on top of the slag. The simulated "open-eye" corresponds to the "splash-zone". The predicted gas stirring in CAS-OB gives an efficient stirring also of the top slag. This was confirmed by noting that slag samples taken from the ladle seem to be representative of the mean slag composition. Finally, streamlines during stirring have been compared with sculling and wear observed in the production ladle. Good agreement was obtained.

Keywords:

Ladle metallurgy, Ladle slag, Numerical simulation, CFD models, Slag flow, sculling, slag sampling, "open-eye", CAS-OB process

Introduction

A good knowledge of the movement and physical behaviour of the liquid phases in the ladle is necessary to understand the kinetics of the slag - steel reactions and slag - lining reactions. A lot of work has been reported on the movement of liquid steel in ladles. [1-58]. The work done is summarized in **Table 1**. The table shows that extensive work has been done on the fluid flow of liquid steel in ladles during holding, teeming and stirring. However, for gas stirring the actual process is a multiphase flow of gas, steel and slag. Incorporating the slag phase makes things more difficult both to calculate and measure, due to a higher and more irregular viscosity of the slag. Some CFD models have been developed for the combined flow of slag, steel and gas [59-65]. However, this case is less studied. A lot of work remains to be done on measurements and on the combination of measurements with simulation.

The aim of this study is to reach an increased knowledge on that subject. The liquid movements in the slag phase are investigated by means of a combination of production plant experiments and CFD simulations. The experimental data are compared with the results of the calculations to validate the models and gain understanding. The paper begins with a short description of the mathematical model. Then three different cases are presented, using both calculation results from the CFD model and plant experiments as well as comparison of experimental and predicted results.

The experimental work was carried out in the steel plant of SSAB Tunnplåt AB in Luleå. The steel is made in two 107-tonne BOF converters. Before tapping, the steel has a temperature of

approximately 1680 °C, a carbon content around 0.005 %C, and an oxygen content of approximately 800 ppm. The steel is tapped into a ladle. Alloys, deoxidants and slag material are added during tapping. The steel is transported to a CAS-OB plant, where ladle treatment is made. The treatment time is approximately 30 minutes. After ladle treatment the steel is transported to a slab caster. The transport time is around 15 minutes and the casting time is approximately 40 minutes per heat.

Theoretical fluid flow model of slag and metal

The theoretical model of the CAS-OB process describes argon injection into a steel bath with a top slag. Thus, the mathematical model includes solutions for three phases: namely the argon, steel and slag. The three-phase model can be used to study the flow conditions in the slag and steel and also around the steel/slag interface during gas stirring.

Complete descriptions of the model and verification are given in previous publications of both the two-dimensional two-phase models for gas stirring in the CAS-OB vessel [38,39,54] and the treatment of the slag phase [60,7]. A brief description is given below.

Mathematical formulation

The following assumptions are made in the statement of the mathematical model:

- a) The CAS-OB vessel is axially symmetric.
- b) The gas bubbles are introduced through a porous plug located in the centre of the ladle bottom.
- c) The calculations are performed using the transient solution mode.
- d) The free surface at the slag/air interface is frictionless and flat. Allowance is made for the escape of gas bubbles at the surface.
- e) An interface-friction coefficient is used to describe the force between the gas and the liquid phases.
- f) There is no heat exchange between steel and the bell or between slag and the bell.
- g) The walls of the bell are frictionless.
- h) At the start of a calculation, there is an equal slag depth everywhere, both inside and outside the bell.
- i) The slag is homogeneous.

According to a), b) and d) above the governing equations can be written in two-dimensional cylindrical coordinates.

Transport equations

The mathematical model describes a general flow variable ϕ , which can, for example, express the density, momentum, enthalpy or species. The conservation of this variable within a finite control volume can be expressed as a balance between various processes, which tend to increase or decrease the value of that variable. This balance leads to a transport equation, which has the following general form according to Patankar [65]:

$$\frac{\partial}{\partial t}(\rho\phi) + \frac{\partial}{\partial x_i}(\rho\phi u_i) = \frac{\partial}{\partial x_i}(\Gamma_\phi \frac{\partial \phi}{\partial x_i}) + S_\phi \quad (1)$$

The first term expresses the rate of change of ϕ with respect to time, the second term expresses the convection (transport due to fluid-flow), the third term expresses the diffusion (transport due to the variation of ϕ from point to point), where Γ_ϕ is the exchange coefficient of the entity

ϕ in the phase and the fourth term expresses the source terms (associated with the creation or destruction of ϕ).

According to the mathematical formulation above the following governing transport equations need to be solved:

- Mass conservation for steel, slag and gas phase
- Conservation of radial momentum for steel, slag and gas phase
- Conservation of axial momentum for steel, slag and gas phase
- Conservation of thermal energy for steel, slag and gas phase
- A modified version of the k- ϵ model to describe turbulence in two-phase systems [66]

Turbulent transport equations

The equations for the turbulent kinetic energy, and the dissipation rate of the turbulent kinetic energy from the well-known k- ϵ model [67] have been used with modified source terms [68].

Friction forces between the gas and the liquid

The friction forces cause the transfer of momentum from the slower moving phase (steel, slag) to the faster moving phase (gas). The friction force per unit volume that the liquid exerts upon the gas at the interface in the axial direction is calculated from a drag coefficient [69], a projected gas area per unit volume and the relative velocity between the gas and liquid phases. The gas bubble size varies in the computational domain and is computed with the "shadow method" [70].

Property variations

The density of argon is calculated using the assumption of an ideal gas. Thus, the gas is compressible. The density, heat capacity and the dynamic molecular viscosity of steel and slag are modelled with temperature dependence [7]

Boundary conditions

The most notably boundary condition is the condition for gas inlet from the porous plug [60]. A separate simulation of the porous plug is made for each gas entry condition, including specific data for each chamber, temperature dependent argon properties and radiation contribution from the steel. A complete description of all boundary conditions is given in a previous publication [7]

Measurement and calculation of "open-eye" in a ladle during gas stirring

The diagram in **Figure 1** shows the result of a multi-phase CFD simulation of gas stirring in a 107 tonne ladle at the CAS-OB plant of SSAB Tunnplåt AB in Luleå. The stirring was made by means of argon gas that was injected through a centrally placed porous plug at the bottom of the ladle. The gas flow in this case was 200 l/min. The diagram shows the distribution of steel and slag in the upper part of the ladle. The diagram shows an "open-eye" with slag free surface at the centre of the ladle. It can be seen that this "open-eye" consists of two parts:

- A central region, where only steel is present. This region is defined as the slag-free zone.

- An outer region, where both slag and steel are present. There is a thin layer of steel on top of the slag, so the steel surface is still slag-free. This region is defined as the splash zone.

The picture in **Figure 2** shows the actual appearance of the "open-eye" during a stirring experiment for the same conditions as those of the simulation in **Figure 1**. The upper surface of the steel and slag in the ladle was photographed. The photograph was taken from the operator's platform through an opening in the exhaust hood. The CAS-OB bell is visible in the upper part of the picture. Contours corresponding to the diameters of the slag-free and splash zones have been included as dotted lines.

The actual diameter of the visible "open-eye" was determined by two methods

- Estimation by an operator.
- Measurement on the photography. This was made by comparing the "open-eye" with a circular steel plate Ø 600mm that was thrown on top of the surface before the experiment. It was photographed with the same camera from the same position as the one used for the pictures of the "open-eye". The photographic image of this reference circle is included in the lower right hand part of the picture.

Contours that correspond to these estimations are included as continuous lines on the photograph. They are also shown in the simulated picture in **Figure 1**. Both visual determinations seem to be closer to the diameter of the splash zone than that of the slag-free zone. This can also be expected, as the upper surface in that region is slag-free.

It is impossible to see the difference between the splash zone and the slag-free zone just by looking on the surface. Everything looks white. However, on the photo in **Figure 2** there seems to be slight variations in the brightness of the steel surface in some parts of the splash zone. This can be due to the fact that the slag surface is not 100 % smooth, and in some places there are "reefs" that reach close to the surface (or penetrate it). The liquid steel on top of such a "reef" is shallow compared to its surroundings and the local surface temperature can be expected to be lower. In a photograph of the surface this can be expected to give an area with less thermal radiation, which looks darker on the photograph.

To make the variations more visible the picture was treated in a commercial graphic program. The brightness and contrast were modified, so that slight variations in the brightness of the steel surface became visible. The result of that modification is shown in the picture on the left hand side of **Figure 3**. The figure shows that the splash zone is speckled with grey areas, whereas the slag-free zone appears to be purely white. After that the same program was used to mark the contours of the darker areas. The result of this operation is shown in the picture on the right hand side of **Figure 3**, where the difference between the surface in the slag-free and the splash area is even more obvious. This result can be looked upon as a confirmation of the general picture shown in **Figure 1**.

The measurements of the "open-eye" in the gas stirring experiment were carried out for four different gas flow rates: 100, 200, 300 and 400 l/min. The CFD simulation of **Figure 1** was also carried out for all four flows and the extension of the slag-free zone and the splash zone was determined. In **Figure 4** these data are shown as a function of the flow rate. The diagram shows that the measured diameter of the "open-eye" increases with increasing gas flow rate. Also there is a very good agreement between the "open-eye" diameter that was measured on

the photograph and the calculated size of the splash area. This seems to confirm that the area that is observed as an "open-eye" is actually the surface of the liquid steel that has been splashed on top of the slag. The diameter estimated by the operators is 30–40 % higher than the one measured on the photography. Otherwise it behaves in a similar way. There is an uncertainty in judging the diameter of the eye by looking through a sampling opening from a platform 5 m above the surface. This is one probable reason for the difference.

An interesting result is that the diameter of the slag free zone seems to be relatively unaffected by the gas flow. Independently of the gas flow there seems to be a hole of approximately 0.4 m through the slag. The main effect when the flow rate increases is that the plume is more intense and causes the steel on top of the slag to splash over a wider area.

The mixing degree of top slag and its effect on the reliability of slag samples.

General

In slag–steel metallurgy the slag is usually looked upon as a homogeneous entity. We talk about "slag composition", and this is based upon a slag sample, which is taken somewhere in the slag. This is true only if the slag is a homogeneous mass, which can be described by one slag composition. However, mixing of liquid slag is more difficult than mixing of liquid steel, because of its higher viscosity. If the slag is not well mixed, a slag sample that is taken in one part of the slag is not representative of the slag composition. For this reason it is important to understand the mixing behaviour of the slag.

CFD modelling of the velocities in the top slag during holding and stirring

CFD models for simultaneous simulation of steel and slag flows have been developed at MEFOS. The diagram in **Figure 5 a** has been calculated using such a model [71]. It shows the temperatures and velocities of steels and slags close to the surface of a ladle corresponding to the practice in the steel plant of SSAB Tunnplåt AB. The diagram indicates that the slag moves slowly at a maximum velocity in the magnitude of 0.5 cm/s. At a constant velocity of 0.5 cm/s a slag element would need approximately 5 minutes to move between the centre and periphery of the ladle. The transport time from tapping to CAS-OB at SSAB Tunnplåt AB is in the magnitude of 20 minutes. It is reasonable to believe that there is a limited amount of mixing during that transport, if the slag in the ladle behaves as in the CFD simulation.

The diagram in **Figure 5 b** shows the calculated velocities in slag and metal during stirring in the CAS-OB station of SSAB Tunnplåt AB in Luleå [7]. The diagram shows that the gas stirring causes an increased movement in the slag phase as well. The maximum velocity seems to be of the magnitude of 20 cm/s, i.e., approximately 40 times higher than those obtained by natural convection. Thus, it can be expected that the gas stirring causes a major improvement in the mixing of the slag.

Use of multiple slag samples for measurement of the mixing degree

The mixing within the slag phase has been studied by using data from an experiment, where several slag samples were taken simultaneously from the top slag. The slag samples were taken by means of a steel tube that was immersed into the liquid slag. The frozen slag sticking on the tube was collected and analysed. The sampling was made on two occasions:

- When the ladle had just arrived at the CAS-OB station. This occurred approximately 20 – 25 min after the BOF tapping. Three simultaneous samples were taken from different parts of the slag cover.
- When the ladle arrived at the slab caster after CAS-OB treatment and a subsequent transport of approximately 10 minutes. In this case it was possible to take four samples per ladle. The sampling position was one sample in each quadrant of the top surface.
- For two ladles a cup sample was taken as a reference during sampling at the slab caster.

The diagrams in **Figure 6 a** and **Figure 6 b** show the reproducibility of the slag samples taken on arrival at the CAS OB plant and at the slab caster, respectively. The diagrams are histograms showing the relative deviation from the mean value of the samples that were taken at the same occasion. The diagrams show data for four elements: P_2O_5 , Al_2O_3 , V_2O_5 , and TiO_2 . The reproducibility is also shown as standard deviations in **Table 2**.

Both the diagrams and the table show that the samples arriving at the slab caster show a very good reproducibility. This indicates that the mixing has been very good. This can also be expected because of the preceding gas stirring, which always occurs before the ladle leaves the CAS-OB.

The reproducibility is less good for the slag samples, which were taken after arrival at the CAS-OB. In this case the mixing of the slag phase before samplings is only due to natural convection during transport plus the stirring during tapping. That mixing seems to be less efficient. This is what could be expected from the low slag velocities in **Figure 5 a**.

Calculated flow pattern during CAS-OB treatment. Comparison with wear and scull formation on the ladle wall

Figure 7 a shows a schematic sketch of the CAS-OB treatment of steel in the ladle. There is a ceramic bell that can be lowered into the bath. Stirring can be made by injection of argon through a porous plug in the bottom of the ladle. At the start of the process the bell is raised in a position above the bath. Argon is injected with a high flow rate, so that an "open-eye" of naked steel without slag occurs in the centre of the ladle. Then the bell is lowered into the "open-eye" and the gas stirring is allowed to continue. The environment inside the bell is a naked bath with a protective atmosphere (argon gas from the stirring). Even alloys that are sensitive to oxidation can be added with a good yield inside the bell. The possibility also exists to heat the steel by oxygen blowing and simultaneous addition of aluminium inside the bell. The steel is heated by means of the exothermic reaction between aluminium and oxygen. The oxygen is blown by means of a ceramically protected lance that is lowered inside the bell. The steel outside the bell is covered with a slag that is expected to be comparatively stagnant and with a limited interaction with the steel.

Streamlines calculated with the CFD model are also included in **Figure 7 a**. The variation in steel velocity can also be estimated from the figure: a high density of streamlines corresponds to a high velocity. The calculation was made for a gas flow rate of 660 l/min and with a slag depth of 9 cm. The immersion depth of the CAS-OB bell was 20 cm. The streamlines show a relatively complicated pattern with 3 loops. A loop with a high steel velocity close to the ladle wall occurs in the lower half of the ladle. In the upper part of the ladle there are two loops with somewhat lower steel velocity close to the ladle wall. In this case the upper loop shows a

comparatively high velocity in the contact area outside the bell. This can cause reactions between the steel and the ladle slag. However, calculations with different parameters show that this phenomenon could be avoided with a deeper immersion of the bell.

The streamlines indicate a region of intense steel flow close to the surface inside the bell. The Al_2O_3 that is produced inside the bell during the chemical heating can be expected to follow the steel flow and enter all three circulation loops. The simulations were started with the same slag depth inside and outside of the bell. After a short gas stirring the slag was transported to the outside, and the main part of the steel inside the bell was free of slag. This indicates that the slag transport is efficient.

During the first year of CAS-OB practice there was a problem with gradual build-up of a massive scull on the ladle wall. The physical shape of this scull is schematically shown in **Figure 7 b**. The sculling is concentrated to the upper half of the contact area between steel and ladle wall. The maximum thickness of the scull in this region was 5 cm. In **Figure 7 a** this corresponds to the region with moderate velocity close to the wall. In the region with high velocity there was lining wear instead of build-up.

To understand the mechanism of scull formation, samples were taken at a ladle relining. The sampling position was halfway up from the bottom and at an angle of approximately 45° relative to the position of the trunnion. A visual examination indicated that the scull was an aggregate of frozen steel and slag. The densities of two relatively big pieces were determined by means of weighing and water dipping. The measured densities were used to determine the metal/slag ratio within the pieces. A content of metallic iron of 21.7 % and 32.7 %, respectively, was calculated. The photograph in **Figure 8** shows the structure of a 25 mm thick piece of scull. The scull seems to be a complex three-dimensional structure of steel (light in the picture) and a slag phase (dark in the picture).

The sample was studied in a SEM EDAX microscope, and the local composition of slag phases was determined. The result indicated that the main component of the slag phase was Al_2O_3 . The analysis also showed some Fe, but it is not possible to find out if this reading was caused by metal phase under the surface or by Fe-oxides in the slag. For this reason no statement is made on the exact Fe-content of the slag phase. In **Figure 9** the local compositions of the slag phase are compared with the 3-phase diagram $\text{CaO}/\text{Al}_2\text{O}_3/\text{SiO}_2$. The composition of the ladle lining is also included for comparison. There was a considerable amount of chemical heating during that period and the compositions in **Figure 9** seem to be comparable to the one expected, if Al_2O_3 created in the bell is transported to the wall and sticks after some reaction with wall lining and/or slag.

Based on these investigations a modified slag and lining practice was developed. The modification involved a slag with a higher CaO content, which could react and dissolve the Al_2O_3 . This was successful and the sculling was eliminated. A spinel lining was also introduced to maximise life of the ladle lining with the new slag practice.

Discussion

“Open-eye” during gas stirring

The simulations indicate that the “open-eye” consists of two zones, shaped as concentric circles. There is an inner slag-free zone and a concentric “splash zone” with steel on top of the slag. The photographic analysis for 200 l/minute in **Figure 3** seems to verify this conclusion. It seems that the area, which is usually looked upon as the “open-eye”, in reality is the outline of the “splash-zone”. In this case the outline of both zones was relatively regular.

In other cases the geometry of the two zones was less regular. This is probably due to the fact that the slag temperature is in a region where small variations in slag temperatures can cause a big local variation in slag properties. Also the slag may be partly solid. However, although the outline of the two regions does not exactly conform to regular concentric circles, it seems that even in these cases the diameter of the visible “open-eye” corresponds to that of the calculated splash zone (**Figure 4**).

Accuracy of the slag sampling

As mentioned above, the standard method for slag sampling at SSAB Tunnplåt AB is to immerse a steel tube and collect the frozen slag that is sticking on the tube. If the slag is not homogeneous and contains both liquid and solid phase, there is a risk that the tube sample contains only the liquid phase. In that case the sample would not be fully representative for the slag. To investigate this, reference samples were taken by a sampling cup simultaneously with the four tube samples. This was made with two of the ladles arriving at the slab caster. The composition of the tube and cup samples is plotted against each other in **Figure 10**.

The diagram shows the following tendency for systematic deviation:

- The iron content is higher in the tube sample.
- The contents of most other elements seem to be lower in the tube sample than in the cup sample (exception: one reading of SiO_2).

Usually, slag with high iron content is more liquid. Thus the result can be looked upon as an indication that the tube method is to some extent selective towards the liquid part of the slag. However, the error seems to be of limited magnitude, and the method seems acceptable for most operational purposes.

Flow pattern during CAS-OB treatment. Comparison with wear and scull formation on the ladle wall

The comparison between **Figure 7 a** and **Figure 7 b** indicates that accumulation occurs where the predicted steel velocity is low, and that wear occurs where it is high. It can be seen that the main flow of steel leaving the interior of the bell approaches the ladle wall just below the observed sculling, with part of the steel entering a re-circulation loop with the steel flow close to the wall directed upwards. Due to the density difference between alumina and steel, most of the alumina will enter this re-circulation loop, where it has a certain residence time. Some of the alumina probably will, for each turn in the re-circulation loop, clad onto the ladle lining. The good connection between the predicted fluid flow and the observed sculling/wear can be looked upon as further details validating the model. In **Figure 7 a** there is also a zone with a high liquid velocity just outside the bell. Practical observations during CAS-OB treatment confirm that there is a visible stirring of the slag in that region. The data available in this study

are not sufficient for a deeper investigation of this phenomenon. A further study would be of interest because of the possible effects on steel quality.

The creation of the sculling at the ladle wall could be caused by at least two reaction mechanisms:

- Al_2O_3 that has been created in the bell reacts with the ladle slag and the product sticks at the ladle wall to create the scull
- The scull is formed by reaction of the ladle lining with Al_2O_3 and some slag droplets

From the 3-component diagram in **Figure 9** it seems that both mechanisms are possible. The data from this study are not sufficient to conclude which of the mechanisms above that is responsible for the observed sculling.

Conclusions

A CFD model for combined calculation of liquid movement in steel and top slag in steel ladles has been used to simulate three different cases:

- Formation of an "open-eye" during gas stirring
- Mixing and fluid flow in the slag phase during holding and gas stirring
- The connection between fluid movement and erosion/sculling

Experiments have been carried out in a 107 tonne ladle and the results have been compared to those of the CFD simulations. In, general, the comparison indicates that the simulation can provide a good prediction of slag behaviour.

The CFD simulations show that the "open-eye" during gas stirring consists of a central slag free region surrounded by a splash zone with steel on top of the slag. The size of the "open-eye" has been measured by photographic method. The visible "open-eye" corresponds to the outline of the predicted splash zone

Further, both the measured and predicted stirring of the slag is weak, i.e. inefficient, during the holding and transport of the ladle before CAS-OB.

On the other hand, both simulations and sampling experiments indicate that gas stirring in the CAS-OB causes a good mixing of the top-slag. Slag samples taken with standard methods in the top slag are representative for the slag composition when the sampling is carried out after the gas stirring.

Finally, observations of wear and sculling zones in the production ladles was found to correspond to zones of high and low predicted velocity in the steel bath close to the ladle wall during CAS-OB treatment. Also, a zone with high velocity outside the bell matches visual observations of intense slag stirring in that region during CAS-OB treatment.

References

1. Jonsson K. O., Dr Eng Thesis in Ferrous Metallurgy at MEFOS 1970. (in Swedish)
2. Wester J Å: Report on Gas stirring trials: MEFOS internal report MF 2/68 1968
3. Reiche K., Köhn W. and Wünnenberg K., Stahl und Eisen 105, 1985 No. 19, pp. 981 - 986
4. Grip C.E., STEELMAKING CONFERENCE PROCEEDINGS, Volume 77, Chicago Il, USA, (1994), pp 103 -115
5. Grip C.E. and Österberg A.K., SCANINJECT VII proceedings, Part II, Luleå, Sweden, (1995), pp 147 - 170
6. Olika B., Pan Y., Björkman B. and Grip C.E., SCANDINAVIAN JOURNAL OF METALS, Vol. 25 (1996), pp 18 - 26
7. Jonsson L., Grip C.E., Johansson A. and Jönsson P., STEELMAKING CONFERENCE PROCEEDINGS, Volume 80, (1997), pp 69-82, Chicago Il, USA
8. Koo Y. S., Kang T., Lee I. R. and Gal H. Y., 1989 Steelmaking Conference Proceedings, pp. 415 – 421
9. C E Grip, Jonsson L, Jönsson P, and Jonsson K O , ISIJ International, Volume 39, no 7, July 1999
10. Grip C E et al, Scandinavian Journal of Metallurgy 2000; 29; 30 -38
11. Grip C E et al, Scanmet 1, Luleå, June 7-8 1999;
12. Grip C.E., Ph D Thesis, Luleå Technical University, Luleå, Sweden, 1998
13. Ilegbusi J. and Szekeley J., Transactions ISIJ, Vol. 27, 1987, pp. 563-569
14. Austin R. et al, ISIJ International, Vol. 32 (1992), No. 2, pp 196-200
15. Chakraborty S. and Sahai Y., Metallurgical Transactions B, Volume 23 B, April 1992, pp. 135-151
16. Grip C. E., Lampinen H.O., Lundqvist M. and Widehult S., ISIJ Int., Vol. 36 (1996), supplement, S211.
17. M Lundqvist, B Sc. Thesis, Kiruna dept. of Luleå Technical University, 1995 (In Swedish)
18. Widehult S, M Sc. Thesis, Luleå Technical University, 1996 (In Swedish)
19. Grip C.E., Jonsson L. and Jönsson P., ISIJ INTERNATIONAL, Vol. 37 (1997), No. 11, pp 1081-1090
20. Pan Y, Grip C E and Björkman B., 82nd Steelmaking conference, Chicago Il, USA, March 22-23 1999.
21. Argyropoulos, S A and Mikrovas, A C, Int. J. Heat Mass Transfer, Vol. 39, No. 3, pp.547-561, 1996.
22. Hsiao, T-C, Lehner, T and Kjellberg, B, Scandinavian Journal of Metallurgy, 9, 1980, pp. 105-110.
23. Iguchi, M, Hosohara, S, Kondoh, T, Itoh, Y and Morita, Z, ISIJ International, Vol. 34, 1994, No. 4, pp.330-337.
24. Iguchi, M, Kawabata, H, Ito, K and Morita, Z, ISIJ International, Vol. 334, 1994, no. 12, pp. 980-985.
25. Iguchi, M, Kondoh, T, Morita, Z, Nakajima, K, Hanazaki, K, Uemura, T and Yamamoto, F, Metallurgical and Materials Transactions B, Vol. 26B, April 1995, p.241.
26. Iguchi, M, Uemura, T, Yamaguchi, H, Kuranaga, T and Morita, Z, ISIJ International, Vol. 34, 1994, No. 12, pp. 973-979.
27. Johansen, S T, Robertson, D G C, Woje, K and Engh, T A., Metallurgical Transactions B, Vol. 19B, October 1988, p. 745.
28. Nilmani, M, and Robertson, D G C, Department of Metallurgy and Materials Science, Imperial College of Science and Technology, London SW7 2BP.
29. Robertson, T and Sabbarwal, A K., British Steel Corporation, Teeside Laboratories.

30. Sahajwalla, V, Castillejos, A H and Brimacombe, J K., Metallurgical Transactions B, Vol. 21B, February 1990, p. 71.
31. Schwarz, M P, Musgrove, A R, Hooper, J D and Dang, P., 1992, 10th PTD Conference Proceedings, p. 123.
32. Schwarz, M P and Zughbi, H D., Chemeca '88, Australia's Bicentennial International Conference for the Process Industries, Sydney, 28-31 August 1988.
33. Aldham, C, Cross, M and Markatos, N C, CHAM Ltd., Wimbledon, London, SW19 and Thames Polytechnic, London, SE18.
34. Cross, M, Markatos, N.C and Aldham, C., CHAM Ltd., Wimbledon, London, SW19 and Thames Polytechnic, London, SE18.
35. Ilegbusi, O J and Szekely, J., Department of Materials science and Engineering, Massachusetts Institute of Technology, Cambridge, MA 02139, USA.
36. Ilegbusi, O J and Szekely, J., ISIJ International, Vol. 30, 1990, No. 9, pp. 731-739.
37. Joo, S and Guthrie, R I L., Metallurgical Transactions B, Vol. 23 B, December 1992, p. 765.
38. Jönsson P. and Jonsson L., *Scand J Met*, 24 (1995), pp.194-206.
39. Jönsson P. and Jonsson L., SCANINJECT VII, Luleå, June 7-8, 1995.
40. Murthy K., G G., ISIJ International, Vol. 29, 1989, No. 1, pp.49-57.
41. Mazumdar, D and Guthrie, I L., ISIJ International, Vol. 34, 1994, No. %, pp.384-392.
42. McNallan, M J and King, T B., Metallurgical Transactions B, Vol. 13B, June 1982, p. 165.
43. Neifer, M, Rödl, S and Sucker, D., Steel Research 64, 1993, No. 1, p. 54.
44. Neifer, M, Rödl, S and Sucker, D., Stahl und Eisen 112, 14 September 1992, No. 9, p. 105.
45. Rödl, S., Stahl und Eisen 115, 15 may 1995, No. 5, p. 97.
46. Schwarz, M P., Mervyn Willis Symposium and Smelting & Refining Course 6-8 July 1992, University of Melbourne, Australia.
47. Schwarz, H P and Koh, P T L, Scaninject IV, 4th International Conference on Injection Metallurgy, Luleå, Sweden, June 11-13, 1986.
48. Schwarz, M P., ISIJ International, Vol. 31, 1991, No. 9, pp. 947-951.
49. Szekely, J, Lehner, T and Chang, C W., Ironmaking and Steelmaking, 1979, No. 6, p. 285.
50. Turkoglu, H and Farouk, B., ISIJ International, Vol. 31, 1991, No. 12, pp. 1371-1380.
51. Turkoglu, H and Farouk, B., Numerical Heat Transfer, Part A, Vol. 21, pp. 377-399, 1992.
52. Zhu, M-Y, Inomoto, T, Sawada, I and Hsiao, T-C., ISIJ International, vol. 35, 1995, No. 5, pp. 472-479.
53. Castillejos E, A H, Salcudean, M E and Brimacombe, J K., Metallurgical Transactions B, Vol. 20B, October 1989, p. 603.
54. "Gas injection into liquid metals", University of Newcastle upon Tyne, Department of Metallurgy and Engineering Materials.
55. Kato, Y, Nakato, H, Fujii, T, Ohmiya, S and Takatori, S., ISIJ International, Vol. 33, 1993, No. 10, pp.1088-1094.
56. Spalding, B D., Computational Fluid Dynamics Unit Imperial College of Science and Technology, London SW7 2AZ, England.
57. Tomazin, C E, Upton, E A and Wallis, R A., Proceedings, Vol. 69, Washington, D.C. USA.
58. Zhuo, M and Brimacombe, J K., Metallurgical and Materials Transactions B, Vol. 25B, Oct 1994, p. 681.
59. Alexis J., Jonsson L. and Jönsson P., Clean Steel 5, 2-4 June 1997, Balatonszeplak, Hungary, Fifth Int'l. Conf. on Clean Steel, Vol. 1, pp. 49-58, 1997

60. Jonsson L. and Jönsson P., ISIJ International, Vol. 36 (1996), No 9, pp. 27-1134.
61. Alexis, J, Jönsson, P G, Jonsson, L., ISIJ International, Vol 39, No. 8, pp. 772-778
62. Hallberg, M, Jonsson, L and Alexis, J., SCANMET I, Luleå, June 7-8, 1999,.
63. Jonsson, L, Du Sichen and Jönsson, P, ISIJ International, Vol. 38, (1998), No. 3, pp. 260-267, Vol 2, pp. 119 - 169
64. Jönsson, P, Jonsson, L and Du Sichen, ISIJ International, Vol. 37, (1997), No. 11, pp. 484-491.
65. S. V. Patankar, Hemisphere Publishing Corp., New York, NY, 1980.
66. Phoenix Ver. 2 "Encyclopaedia", CHAM Ltd, London (1994).
67. Launder B. E and Spalding D.B.: Mathematical Models of Turbulence, Academic Press, London, England, (1972).
68. Mostafa A.A. and Mongia H.C.: Int J Heat Mass Transf, 10 (1988), 2063
69. Clift R., Grace J.R., and Weber M.E.: Bubbles, Drops and Particles, Academic Press, New York, USA, (1989).
70. Spalding D.B.: 19th Symp Combustion, The Combustion Inst, (1982), 941.
71. Solhed H. et al, Scanmet 1, 7-8 June 1999, SCANMET I, Luleå, June 7-8, 1999, Vol 2, pp. 65-85
72. Slag Atlas, 2nd Edition, Verlag Stahleisen GmbH, Düsseldorf, 1995 Slag Atlas, 2nd Edition, Verlag Stahleisen GmbH, Düsseldorf, 1995

Tables

Table 1 Summary of previous investigations on movement of liquid steel and slag in ladles. The numbers refer to position in the reference list. The area covered by this study is shown schematically.

	Experimental work in steel ladle or model	CFD Simulation
<i>Flow in one liquid phase (steel)</i>		
Thermal stratificaton	1- 13	6-15
Drainage flow	9-12, 15-20	9-12, 14-15, 19- 20
Stirring	21-32	31,32-58
<i>Multiphase flow (liquid steel + slag)</i>		
Stirring	65	59-65
<div style="text-align: center;"> <p>This study</p> </div>		

Table 2 Reproducibility of slag samples. Relative standard deviation in % of the mean value.

Oxide	Arrival at CAS	Arrival at Slab Caster
P ₂ O ₅	13	5,5
Al ₂ O ₃	9	2,5
V ₂ O ₅	12	2,8
TiO ₂	10	2,8

Pictures

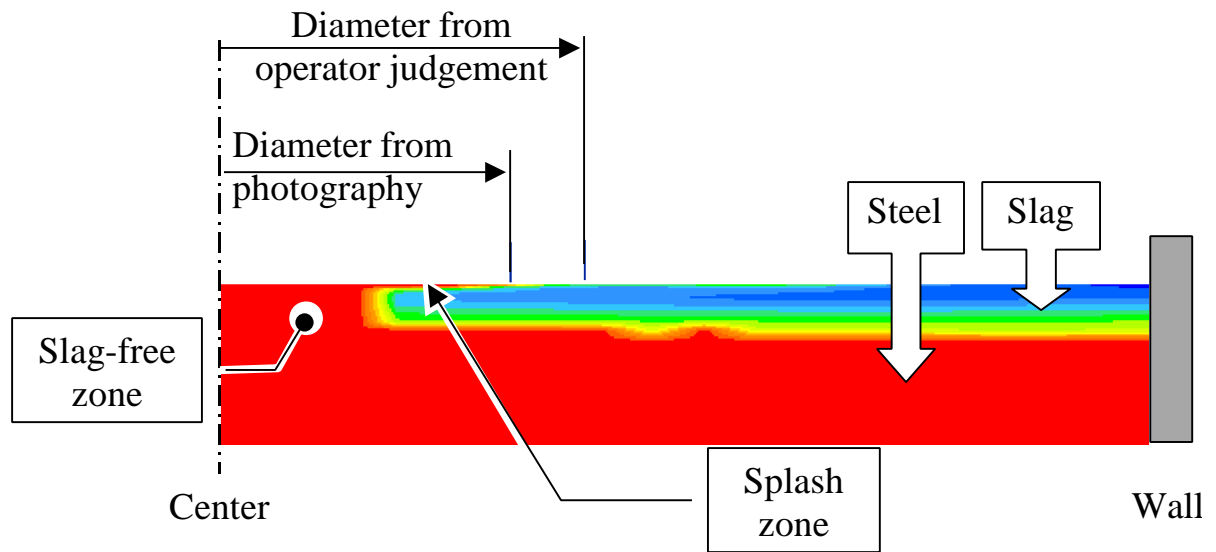


Figure 1 CFD simulation of gas stirring in a 107-tonne ladle. Gas flow 200 l/min. Distribution of steel and slag close to the surface of the ladle. The diameters of the "open-eye" from operator estimation and by measurement on a photography are included for comparison

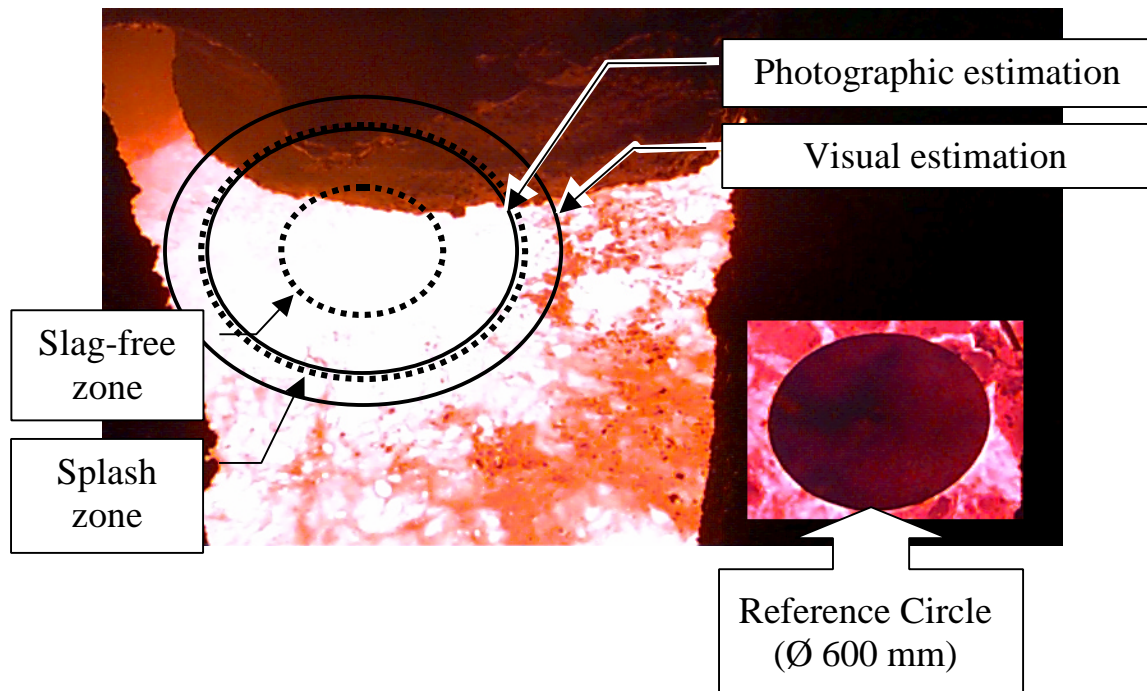


Figure 2 Photography of the "open-eye" during gas stirring in a 107-tonne ladle in the CAS -OB station of SSAB Tunnpå AB. The diameter of the slag-free zone and the splash zone from the CFD simulation is shown as dotted lines. The diameters of the "open-eye" from operator estimation and photographic measurement are shown as continuous lines. A photo of the circular plate that was used as a reference diameter is included in the picture. The stirring was made by argon gas (200l/min) through a porous plug in the bottom of the ladle.

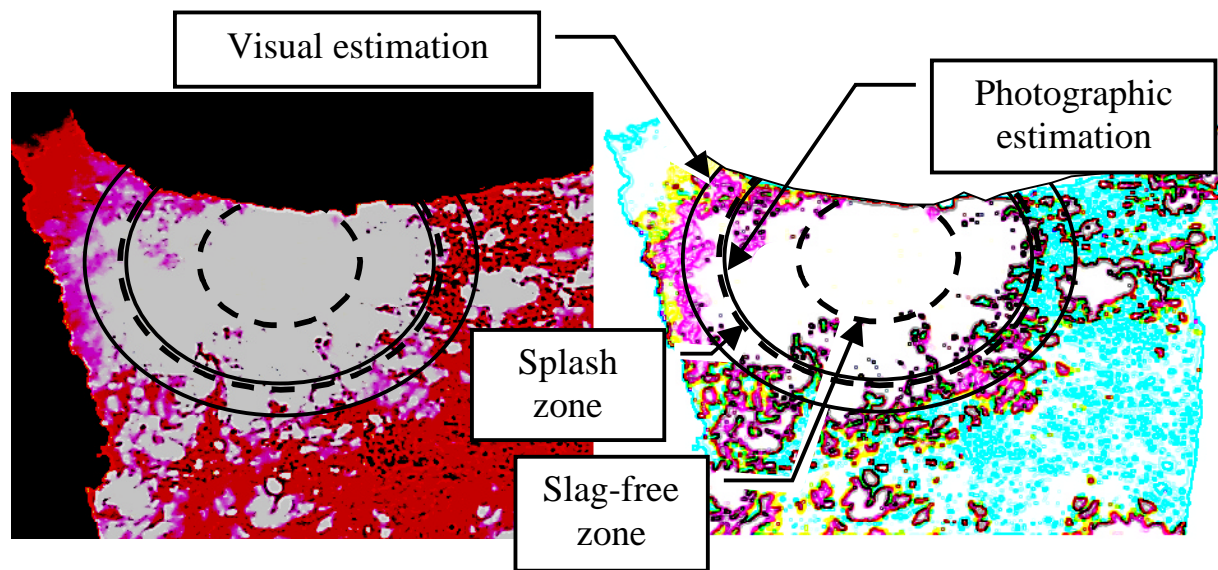


Figure 3 Computer modification of the picture in Figure 2 to visualise the details of the splash zone. In the left hand picture the contrast and brightness have been adjusted. In the right hand picture the contours of the now visible darker areas are shown.

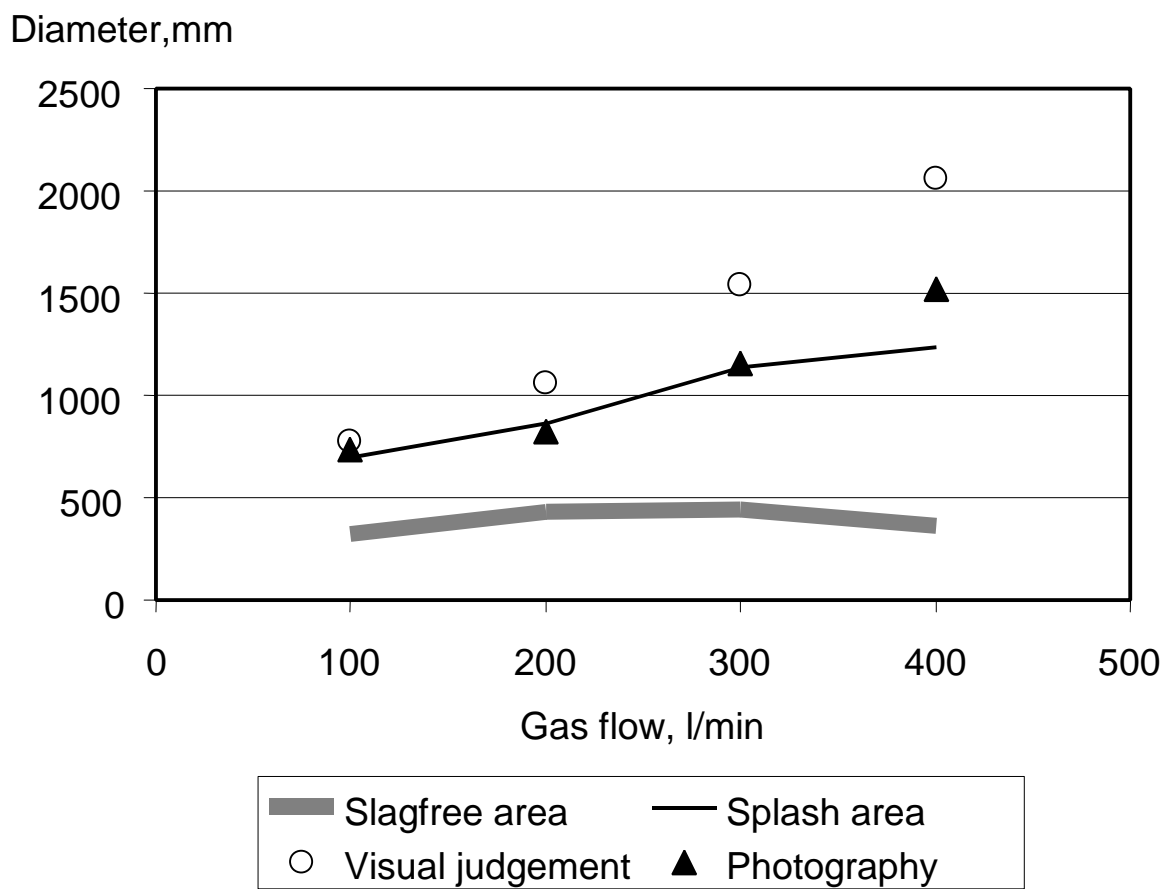
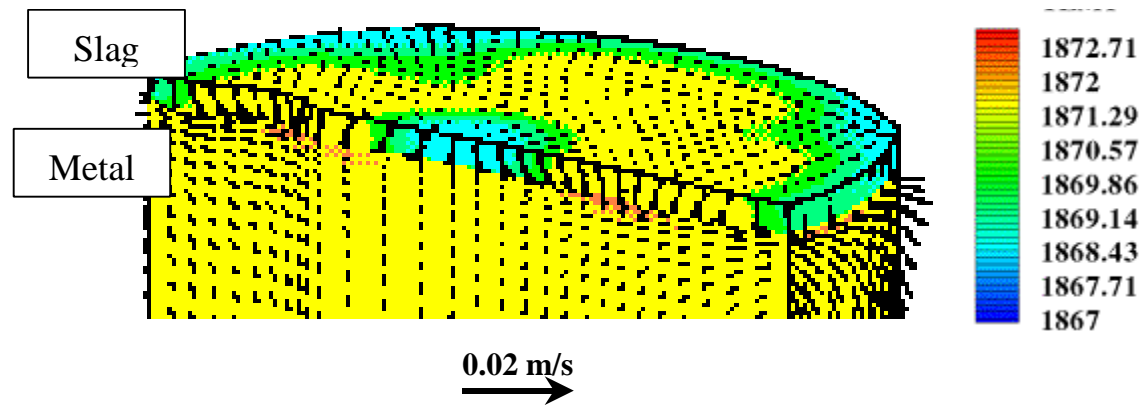
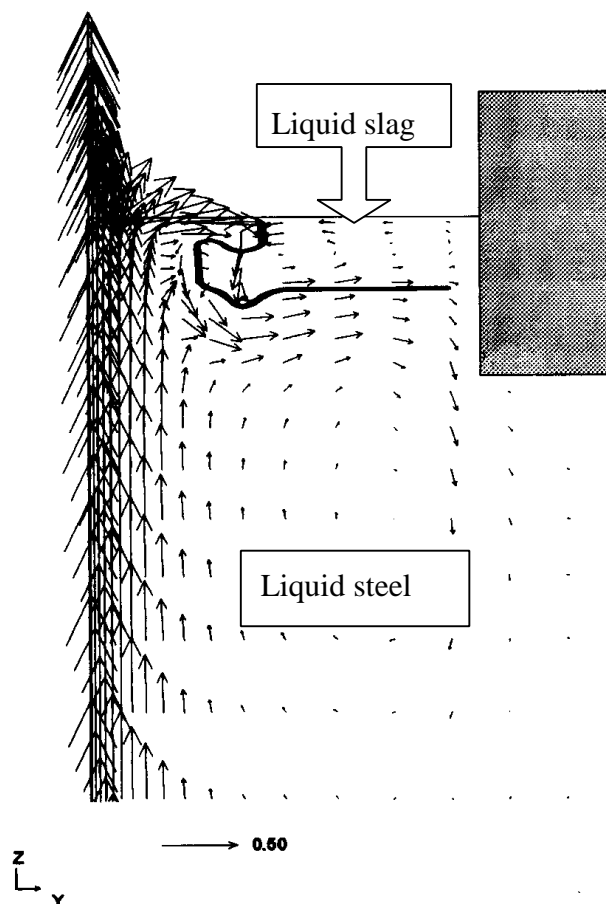


Figure 4 Influence of the flow rate of the stirring gas on the size of the "open-eye" during gas stirring in a 107-tonne ladle.



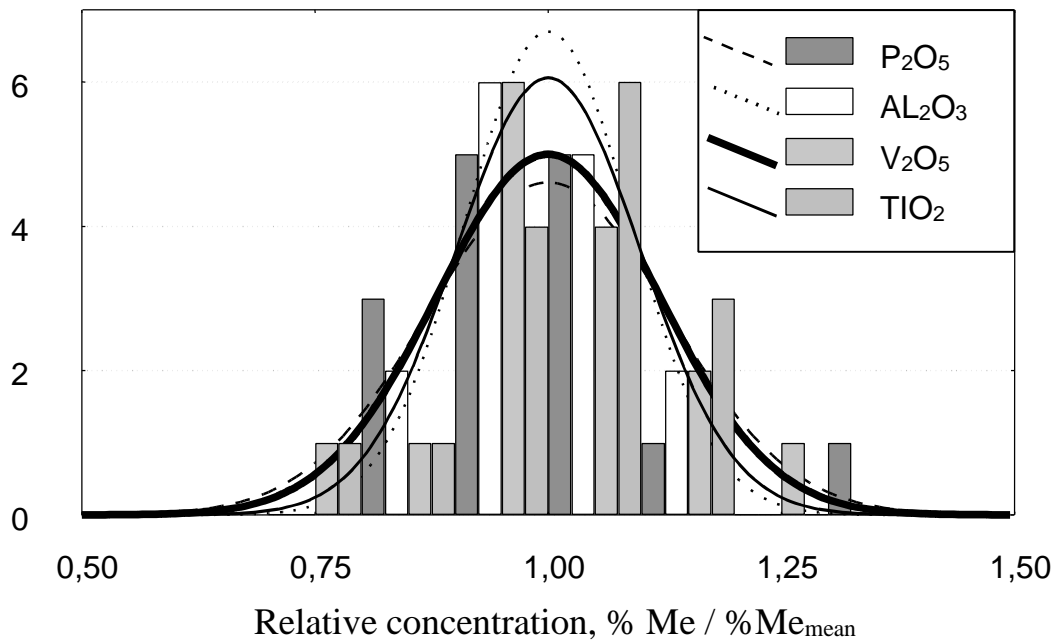
a) Distribution of temperatures and velocities in ladle slag resulting from natural convection [71]



b) Distribution of and velocities in steel and slag during gas stirring in CAS-OB [7]

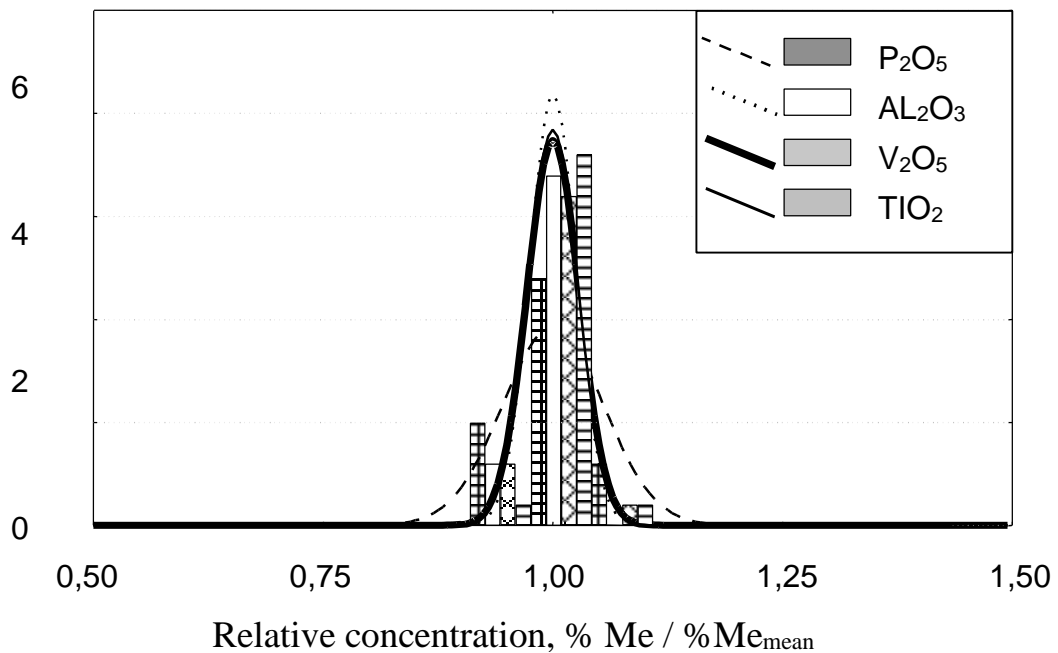
Figure 5 Velocities in steel and slag phase during holding and gas stirring. The velocities have been calculated by means of CFD simulation of steel and slag in a 107- tonne ladle.

Number of observations



a) Sampling on arrival at CAS-OB

Number of observations



b) Sampling on arrival at CC

Figure 6 Reproducibility of slag sampling. Deviation between slag samples taken simultaneously from different points at the top surface of the ladle. Sampling method: dipping of a thin steel tube.

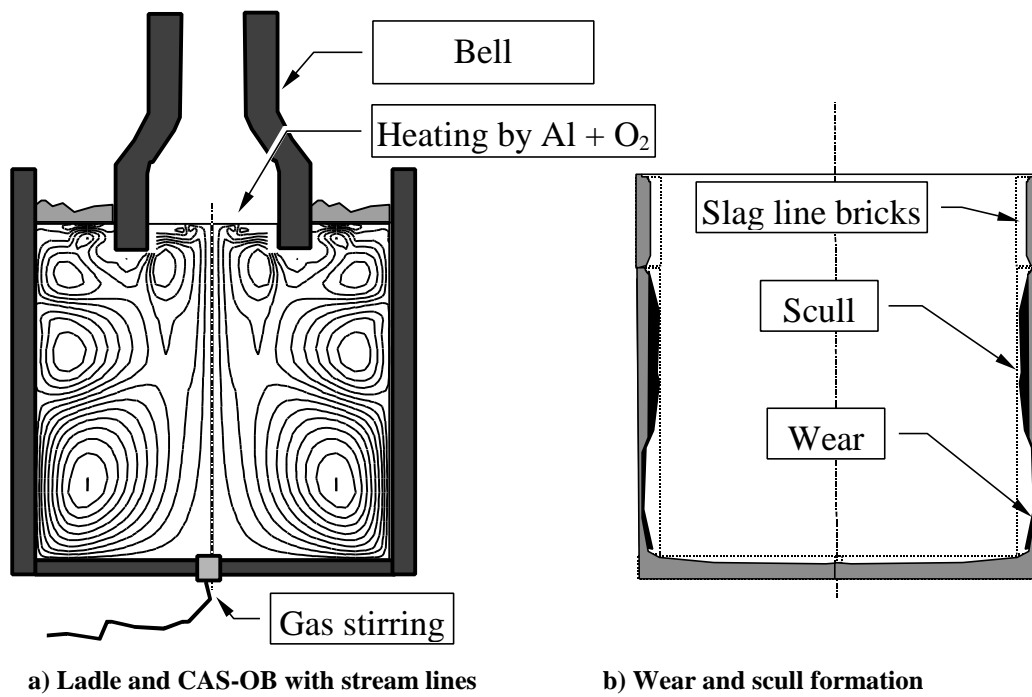


Figure 7 Comparison of calculated stream lines [7] during CAS-OB treatment with wear and scull formation observed at the ladle wall.

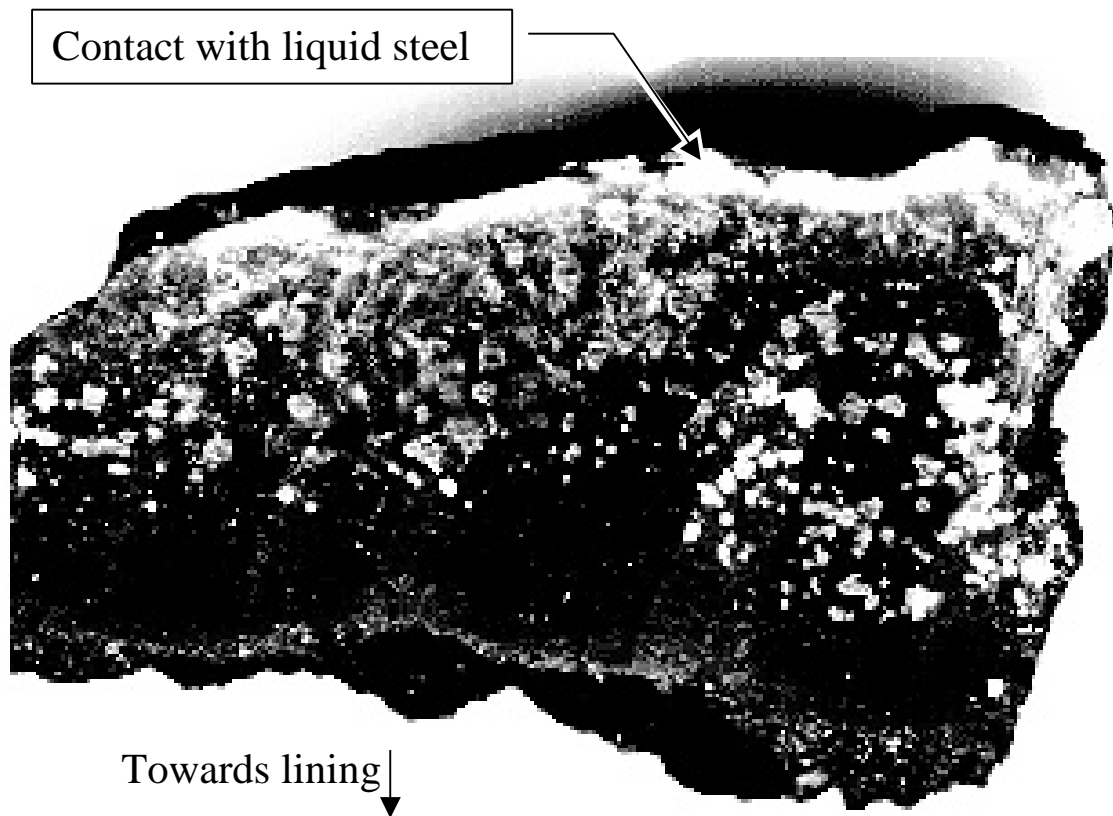


Figure 8 Structure of slag scull. The figure shows a sample of a ladle scull taken from the upper half of a ladle during relining. The dark phase is slag or ceramics and the light phase is metal.

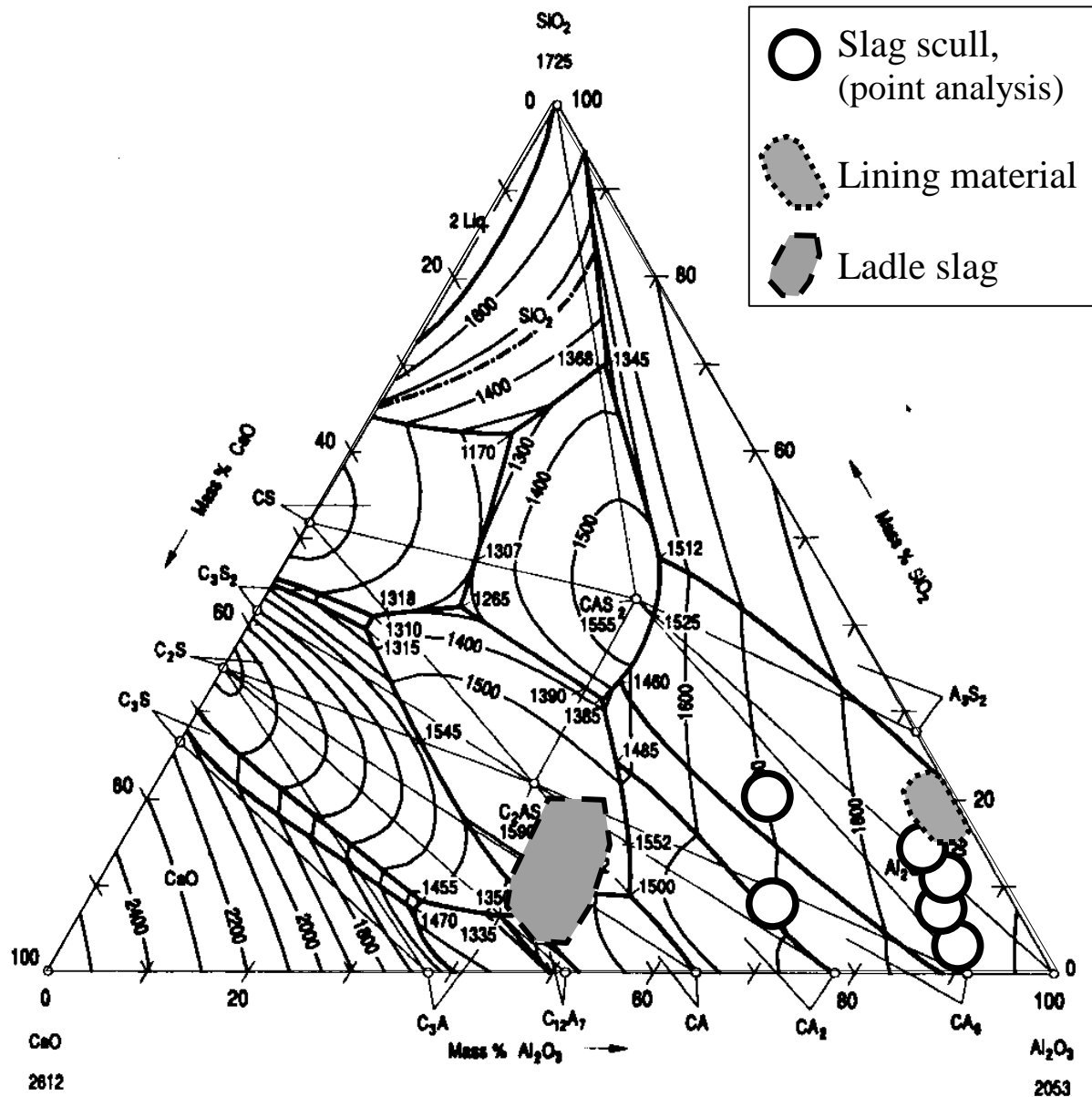


Figure 9 Composition of the slag phase in the scull of Figure 8. The phase diagram CaO - SiO₂- Al₂O₃ [72] is included as a reference. The data points show compositions measured with a SEM - EDAX microscope at different points in the slag phase. The value on the CaO axis corresponds to (%CaO+%MgO) in the slag. The normal composition of the ladle slag after CAS-OB and that of the ladle lining are included for comparison.

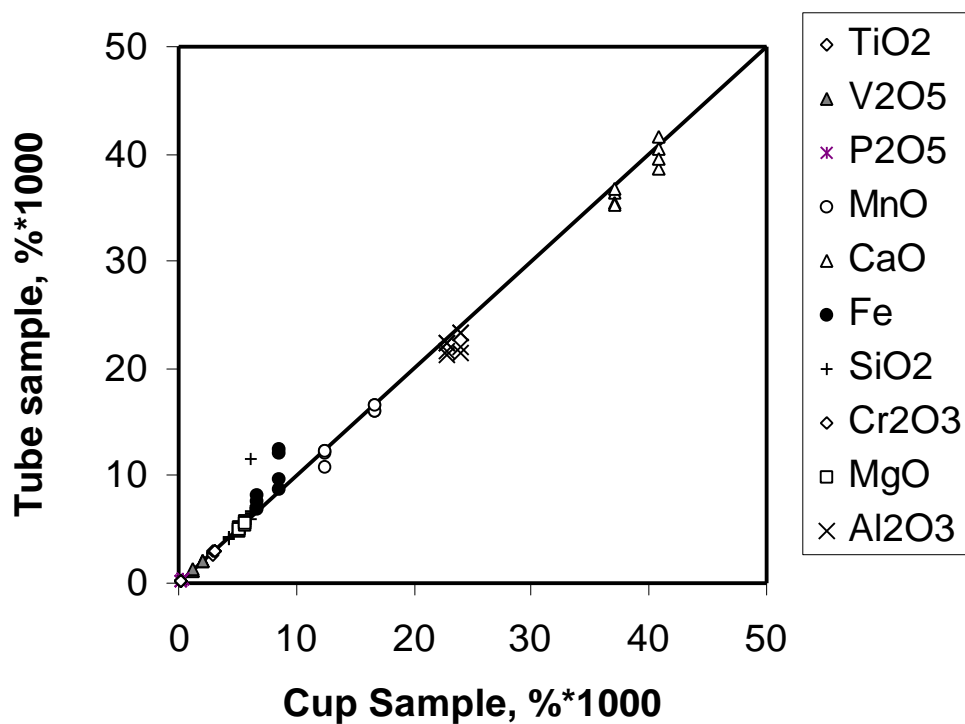


Figure 10 Comparison of slag samples taken by dipping of a steel tube to a sample that was taken from the same ladle by means of a sampling cup. Data from two heats are included. For each heat 4 tube samples and one cup sample are studied.

